Published in final edited form as:
Virology. 2011 October 25; 419(2): 72–83. doi:10.1016/j.virol.2011.08.009.

The Ebola virus glycoprotein mediates entry via a non-classical dynamin-dependent macropinocytic pathway

Nirupama Mulherkar[1], **Matthijs Raaben**[2], **Juan Carlos de la Torre**[3], **Sean P. Whelan**[2], and **Kartik Chandran**[1,*]

[1] Department of Microbiology and Immunology, Albert Einstein College of Medicine, Bronx, NY 10461

[2] Department of Microbiology and Molecular Genetics, Harvard Medical School, Boston, MA 02115

[3] Division of Virology, Department of Neuropharmacology, The Scripps Research Institute, La Jolla, California 92037

Abstract

Ebola virus (EBOV) has been reported to enter cultured cell lines via a dynamin-2-independent macropinocytic pathway or clathrin-mediated endocytosis. The route(s) of productive EBOV internalization into physiologically relevant cell types remain unexplored, and viral-host requirements for this process are incompletely understood. Here, we use electron microscopy and complementary chemical and genetic approaches to demonstrate that the viral glycoprotein, GP, induces macropinocytic uptake of viral particles into cells. GP's highly-glycosylated mucin domain is dispensable for virus-induced macropinocytosis, arguing that interactions between other sequences in GP and the host cell surface are responsible. Unexpectedly, we also found a requirement for the large GTPase dynamin-2, which is proposed to be dispensable for several types of macropinocytosis. Our results provide evidence that EBOV uses an atypical dynamin-dependent macropinocytosis-like entry pathway to enter Vero cells, adherent human peripheral blood-derived monocytes, and a mouse dendritic cell line.

Keywords

Ebola virus; filovirus; vesicular stomatitis virus; virus-like particles; glycoprotein; viral entry; viral infection; endocytosis; macropinocytosis; Pak-1; dynamin; antigen presenting cells; monocytes; dendritic cells

Introduction

Filoviruses are filamentous enveloped viruses with nonsegmented negative-sense RNA genomes. All known filoviruses belong to one of three genera: *Ebolavirus*, consisting of the five species *Zaire ebolavirus*, Tai Forest ebolavirus, Bundibugyo ebolavirus, Sudan

*Corresponding author Kartik Chandran, PhD. 1300 Morris Park Avenue, Bronx, NY 10461 kartik.chandran@einstein.yu.edu Tel: 718-430-8851 Fax: 718-430-8850.

ebolavirus, and *Reston ebolavirus; Marburgvirus*, consisting of the species *Marburg marburgvirus; and Cuevavirus*, consisting of the species *Lloviu cuevavirus* (tentative) (Kuhn et al., 2010). Ebola virus (EBOV), the type member of the species *Zaire Ebolavirus*, is responsible for recurring outbreaks of hemorrhagic fever in humans and non-human primates (Ascenzi et al., 2008; Feldmann et al., 2007; Kuhn, 2008).

The EBOV glycoprotein, GP, mediates all of the steps in viral entry into host cells, including fusion between viral and cellular membranes (Takada et al., 1997; Wool-Lewis and Bates, 1998). GP-dependent viral entry requires endosomal acid pH and GP proteolytic cleavage by endo/lysososomal cysteine proteases, suggesting that viral membrane fusion and cytoplasmic escape occur from a late endo/lysosomal compartment (Chandran et al., 2005; Sanchez, 2007; Schornberg et al., 2006; Wong et al., 2010; Yonezawa et al., 2005). However, the specific pathways by which EBOV particles are internalized and delivered to these intracellular sites of membrane fusion remain incompletely defined. Early studies aimed at deciphering the EBOV internalization route indicated a requirement for an active actin and microtubule cytoskeleton (Sanchez, 2007; Yonezawa et al., 2005). Other studies implicated clathrin- and caveolin-dependent endocytic pathways in EBOV entry (Bhattacharyya et al., 2010; Sanchez, 2007). More recently, Quinn and co-workers showed that a RhoC-dependent pathway is involved in the uptake of vesicular stomatitis virus (VSV) pseudotypes bearing EBOV GP (Quinn et al., 2009).

While our current manuscript was in preparation, two groups demonstrated a critical role for macropinocytosis in mediating EBOV entry into several cultured cell lines. These investigators also ruled out a role for clathrin-mediated endocytosis (Nanbo et al., 2010; Saeed et al., 2010). Furthermore, work by Nanbo and co-workers suggested that an interaction between EBOV GP and an unknown host cell factor induces viral uptake by macropinocytosis (Nanbo et al., 2010). Multiple ceArf6ll-surface factors have been reported to be involved in EBOV entry, including TIM-1 (T cell immunoglobulin and mucin domain 1), DC-SIGN, folate receptor-α, C-type lectins, mannose binding lectin and integrin β_1 (Alvarez et al., 2002; Chan et al., 2001; Ji et al., 2005; Kondratowicz et al., 2011; Simmons et al., 2003b; Takada et al., 2000). A recent study also indicated a role for the Tyro3 receptor kinase Axl in enhancing EBOV macropinocytosis in a cell-type dependent manner (Hunt et al., 2011). However, the mechanism(s) of induction of macropinocytosis in permissive cells by EBOV GP and the role of specific domains of GP in mediating this function remain unclear. In this study, we confirm and extend the previous observations that EBOV GP-dependent viral entry requires a macropinocytosis-like uptake pathway. We provide new evidence for this entry mechanism by electron microscopy, and show it is relevant not only in cultured fibroblast cell lines but also in physiologically relevant antigen-presenting cell types. We demonstrate that viral internalization by macropinocytosis is induced by the viral glycoprotein GP, but that the highly glycosylated and surface-exposed GP mucin-like domain previously implicated in viral attachment (Lin et al., 2003; Simmons et al., 2003a; Simmons et al., 2002; Takada et al., 2004) is dispensable for this process. Finally, our work reveals an unexpected dependence of filovirus entry on the large GTPase dynamin-2 that is independent of clathrin-mediated endocytosis.

Results

Viral entry into Vero cells mediated by EBOV GPΔMuc is restricted by macropinocytosis inhibitor EIPA

Based on the predicted pre-fusion structure of full length EBOV GP (Lee et al., 2008; Lee and Saphire, 2009), the mucin-like domain (Muc) exists as an external domain shielding the GP1 and GP2 subunits of EBOV GP. This raised the possibility that the Muc might have a role in inducing uptake via macropinocytosis in addition to its role in immune evasion

(Simmons et al., 2002; Wilson et al., 2000). Also, Muc incorporates five N-linked and 12-17 O-linked glycans (Lee and Saphire, 2009) that could potentially interact with EBOV co-receptors/adhesion molecules such as mannose binding lectin, C-type lectins and integrins to induce macropinocytic uptake (Ji et al., 2005; Takada et al., 2000). Accordingly, we tested the effect of macropinocytosis inhibitor EIPA (Koivusalo et al., 2010) on EBOV GPΔMuc dependent entry in Vero grivet monkey cells. We pretreated Vero cells with EIPA and then exposed the cells to vesicular stomatitis virus (VSV) pseudotypes expressing either the VSV G protein (VSV-G) or EBOV GPΔMuc (VSV-GPΔMuc) (Fig. 1A). As observed previously for full length EBOV GP (Nanbo et al., 2010; Saeed et al., 2010), EIPA inhibited infection by VSV-GPΔMuc but not VSV-G. EIPA also inhibited cytoplasmic entry by virus-like particles (VLPs) bearing EBOV GPΔMuc and a VP40–β-lactamase fusion protein (βLaM-VLPs) (Fig. 1B). We next directly examined the effect of Muc deletion on the pathway of viral uptake (Fig. 1C). To monitor viral attachment, EBOV GPΔMuc VLPs bearing an eGFP-VP40 fusion protein (eGFP-VLPs) were exposed to Vero cells at 4°C, and cell-associated eGFP fluorescence was measured by flow cytometry. To monitor viral uptake, cells with bound VLPs were warmed to 37°C for 30 min, acid-washed to remove any VLPs that remained at the cell surface, and analyzed by flow cytometry. As shown in figure 1C, EIPA had little or no effect on attachment of VLPs but substantially reduced their internalization into cells. Similar results have been observed with full length EBOV GP (Nanbo et al., 2010; Saeed et al., 2010)(data not shown). We also examined viral uptake by confocal fluorescence microscopy (Fig. 1D). In untreated Vero cells exposed to eGFP-VLPs, the majority of fluorescent puncta localized to the cell interior by 30 min at 37°C, indicating that extensive viral internalization had occurred. By contrast, in cells treated with EIPA, most eGFP fluorescence was associated with the cellular membrane at the same time point. Therefore, EIPA inhibits EBOV GPΔMuc dependent viral uptake into Vero cells. The same concentration of EIPA also efficiently blocked fluid-phase mediated uptake of fluorescently labeled high molecular weight dextran (Fig. 1E). These findings suggest that like full length GP, EBOV GPΔMuc mediates viral uptake into Vero cells predominantly via a macropinocytosis-like pathway.

EBOV GPΔMuc VLPs colocalize with and induce the uptake of fluid phase uptake markers

Uptake of labeled dextran at early time points is known to occur via macropinocytosis. We therefore tested whether EBOV VLPs and labeled dextran can co-exist in the same vesicles. As observed in figure 2A, as early as 10 min, RFP-fused EBOV VLPs colocalized with FITC-labeled dextran, thereby indicating that EBOV VLPs are taken up in the same endocytic compartment as FITC-dextran. The Pearson's coefficient for colocalization in this case was deduced as 0.84. It is well known that macropinocytosis is mediated by ruffling of cellular membranes (Mercer and Helenius, 2009; Mercer et al., 2010) and agents that are internalized by macropinocytosis can induce the uptake of FITC-dextran. Hence we next determined whether incubation with VLPs expressing GPΔMuc could induce uptake of FITC-dextran, as is known for full length GP (Nanbo et al., 2010; Saeed et al., 2010). Pre-exposure to EBOV VLPs could induce uptake of FITC-dextran similar to the positive control phorbol-12-myristate-13 acetate (PMA) in Vero cells (figure 2B). These results indicate that GPΔMuc can activate cellular activities that result in increased uptake of fluid phase markers.

Viral particles bearing EBOV GPΔMuc induce plasma membrane ruffling

We used electron microscopy to further characterize the uptake mechanism of viral particles bearing EBOV GPΔMuc. In contrast to clathrin-mediated uptake of rVSV-G, rVSV-GPΔMuc induces membrane ruffling, which is characteristic of macropinocytosis (figure 3A). Macropinocytic uptake of rVSV expressing EBOV GPΔMuc particles was observed as early as 15 min post inoculation of Vero cells. Similar events are observed at 30 min post

virus exposure (figure 3B). These results further corroborate that uptake of EBOV is primarily mediated by macropinocytosis and that the Muc is dispensable for macropinocytic uptake.

Actin, myosin and PKC inhibitors can inhibit EBOV GPΔMuc-mediated viral uptake and infection in Vero cells

We then tested the effect of other known inhibitors of macropinocytosis (Mercer and Helenius, 2009; Mercer et al., 2010) on EBOV GPΔMuc-dependent entry. Treatment of Vero cells with PKC inhibitor (rottlerin), actin polymerization inhibitor (latrunculin A) and myosin light chain kinase inhibitor (ML9) selectively inhibit infection mediated by EBOV GP but not VSV-G (figure 4A). These compounds also inhibited entry of EBOV GPΔMuc VLPs in the β-lactamase assay (figure 4B). Moreover, all of these inhibitors acted at the uptake step and did not affect binding (figure 4C), which was also confirmed by fluorescence microcopy (Figure 4D). The myosin motor inhibitor, blebbistatin, however, did not have any effect on EBOV infection in Vero cells (figure 4). These findings demonstrate that abrogation of protein kinase C (PKC), actin and myosin light chain kinase inhibits EBOV GPΔMuc uptake in Vero cells, thereby lending support to the possibility that like full length GP, EBOV GPΔMuc enters Vero cells predominantly via a macropinocytosis-like pathway.

Pak-1 but not Arf6 plays an important role in EBOV GPΔMuc-mediated entry into Vero cells

An important cellular factor involved in EBOV macropinocytosis in Vero cells is p21 activated kinase (Pak-1) (Nanbo et al., 2010; Saeed et al., 2010). Expression of the Pak-1 AID (auto-inhibitory domain) significantly inhibits ($P<0.001$) VSV-GPΔMuc infection of Vero cells, whereas expression of the wild type Pak-1 and Pak-1-L107F AID (control) have no effect. Pak-1 AID also reduced uptake of EBOV VLPs as well as FITC-dextran into Vero cells (figure 5B). These results show that like full length GP, EBOV GPΔMuc uptake in Vero cells is regulated by Pak-1.

Arf6 GTPases are known to modulate macropinocytosis in a cell-type dependent manner (Donaldson, 2003; Mercer and Helenius, 2009; Mercer et al., 2010). We investigated the effect of expression of dominant negative Arf6 on EBOV GPΔMuc infection to determine whether the Muc can influence other mediators of macropinocytic uptake. Our results indicate that while expression of Arf6 DN reduced uptake of FITC-dextran, it had no effect on EBOV GPΔMuc infection as well as uptake (figure 5C and D). These results suggest that the macropinocytic pathway mediating EBOV GPΔMuc entry in Vero cells does not involve Arf6.

Dynasore inhibits EBOV GP-dependent infection by interfering with viral entry

The macropinocytic pathway employed by EBOV GP (full length) is proposed to be independent of the large GTPase dynamin (Nanbo et al., 2010; Saeed et al., 2010) and is believed to utilize C-terminal binding protein-1 (CtBP1) for the scission of vesicles (Liberali et al., 2008; Saeed et al., 2010). To determine what, if any, role dynamin plays in entry mediated by EBOV GPΔMuc, we examined the effect of dynamin inhibitors on infection by VSV-GP infection. Infection of both VSV-G and VSV-GPΔMuc was sensitive to dynasore treatment; VSV-GPΔMuc was comparatively more sensitive (figure 6A). In order to rule out the influence of VSV core and also deletion of the mucin-like domain, we performed the same experiment using a dynamin-independent (Quirin et al., 2008) VSV pseudotyped with LCMV glycoprotein (GP) and VSV pseudotyped with full length EBOV GP. As expected, dynasore treatment did not affect LCMV-GP expressing VSV but inhibited only EBOV GP and VSV-G pseudotypes (figure 6B). Consistent with these findings, dynasore also inhibited cell entry by EBOV VLPs (figure 6C). To determine more precisely where such particles

were blocked, we imaged the location of eGFP-VLPs. We found that although dynasore inhibited uptake of Alexa-647-transferrin (figure 6D), it did not block the uptake of EBOV VLPs as measured by flow cytometry (figure 6E). However, as observed in figure 6F, treatment with dynasore leads to more EBOV VLPs associating with the cellular membrane (stained with rhodamine-WGA). Because our biochemical assay of viral uptake depends on the stripping of cell-surface VLPs by acid treatment, we speculate that dynasore arrests EBOV uptake at a later step than EIPA: a step at which the VLPs are protected from extracellular acid.

Role of dynamin-2 in EBOV GP-dependent infection and uptake

To independently verify that dynamin function was required for EBOV infection, we tested the effect of expression of a dominant negative dynamin-2 on infection of EBOV GPΔMuc in Vero cells. Expression of dynamin-2-K44A reduces infection of VSV-GP pseudotypes in a highly reproducible manner (P=0.0004) (figure 7A) as well as EBOV VLPs (figure 7B). As expected, dynamin-2-K44A expression inhibits uptake of transferrin (figure 7C) and leads to an accumulation of EBOV VLPs at the cellular membrane (figure 7D. The EBOV VLPs also colocalize with endogenous dynamin (figure 7E; panel 2) (Pearson's coefficient 0.52). Though some endogenous dynamin-2 co localized with transferrin (panel 3, Pearson's coefficient 0.48) EBOV VLPs did not colocalize with transferrin (panel 4, Pearson's coefficient 0.02). These results indicate that EBOV VLPs and transferrin are not in the same vesicle (Hewlett et al., 1994; Saeed et al., 2010) and that some EBOV VLPs are internalized in a subset of dynamin-2 positive vesicles.

Effect of macropinocytosis inhibitors and dynasore on EBOV GP-dependent infection in antigen presenting cells

Macrophages and dendritic cells are proposed to be the first cell types infected by EBOV upon infection of the host (Bray and Geisbert, 2005; Geisbert et al., 2003). Accordingly, we next tested the effect of dynasore, EIPA, rottlerin, latrunculin A and ML9 on EBOV infection in the Jaws mouse dendritic cell line and in primary human adherent peripheral blood-derived monocytes. Both EIPA and dynasore inhibited VSV-GP (full length and GPΔMuc) pseudotype infection in both cell types (figure 8A and 8B). These results demonstrate that EBOV entry into physiologically-relevant primary cells is also mediated by an atypical dynamin-dependent macropinocytosis-like pathway.

Discussion

EBOV GPΔMuc is necessary and sufficient for macropinocytic uptake

Most viruses exploit cellular endocytic pathways to infect host cells. One well-characterized mode of endocytosis is the clathrin-mediated endocytic (CME) pathway (Conner and Schmid, 2003). Some studies have shown CME to have little or no role in EBOV cell entry (Nanbo et al., 2010; Saeed et al., 2010), whereas some others have implicated CME in a cell type dependent manner (Hunt et al., 2011) and in entry of HIV pseudoparticles expressing EBOV GP (Bhattacharyya et al., 2010; Hunt et al., 2011). Recently, two studies have suggested a predominant role for macropinocytosis in the uptake of EBOV (Nanbo et al., 2010; Saeed et al., 2010). Macropinocytosis is initiated by an external stimulus resulting in activation of receptor tyrosine kinases (Mercer and Helenius, 2009; Mercer et al., 2010). Consistent with previous reports (Hunt et al., 2011; Nanbo et al., 2010; Saeed et al., 2010) our results have also implicated EBOV GP in activating macropinocytic uptake in host cells. While the specific cellular determinant/s involved in EBOV GP-induced macropinocytosis are unknown, potential GP binding partners, including TIM-1, integrin-β1 and mannose-binding lectins (Alvarez et al., 2002; Chan et al., 2001; Ji et al., 2005; Kondratowicz et al., 2011; Nanbo et al., 2010; Saeed et al., 2010; Simmons et al., 2003b; Takada et al., 2000)

may play a role. Additionally, Axl, a member of the Tyro3 protein kinase family could facilitate GP-mediated and GPΔMuc-mediated macropinocytic uptake in a cell type-dependent manner without directly interacting with GP (Brindley et al., 2011; Hunt et al., 2011). Based on its predicted three-dimensional structure, full-length GP is covered by a thick cloak of glycans that include a bulky mucin-like domain, glycan cap and additional N-linked glycans on the sides (Lee et al., 2008; Lee and Saphire, 2009). Indeed, N-linked and O-linked glycans are known to have roles in endocytosis (Ohtsubo and Marth, 2006). We therefore investigated the role of the mucin-like domain (which constitutes both N- and O-linked glycans) in influencing uptake of EBOV via macropinocytsis and/or CME. Our results indicate that deletion of the mucin-like domain neither impairs macropinocytic uptake of EBOV in Vero cells (Figs 1-5, Supplementary Fig 1) nor increases virus uptake by CME as determined by little or no colocalization of EBOV GPΔMuc VLPs with labeled transferrin (figure 7E). Therefore, studies aimed at determining the role of other domains/residues of GP in mediating entry by macropinocytosis are warranted.

Role of actin, PKC and myosin in EBOV entry

Macropinocytosis is characterized by vigorous plasma membrane activity in the form of ruffles. Ruffles are formed by outward-directed actin polymerization and contain several regulators of actin polymerization, disassembly, stabilization and cytoskeletal membrane attachment. Some of these regulators include Arp2/3, VASP, WAVE, PKC and several classes of myosin(Mercer and Helenius, 2009). Our EM data (figure 3) conclusively show that uptake of EBOV GPΔMuc occurs via cellular protrusions/ruffles. Our results using inhibitors of actin polymerization, PKC, myosin II, and macropinocytosis (figures 1 and 4) lend further support to the hypothesis that uptake of EBOV GPΔMuc requires mediators of macropinocytosis. Intriguingly, an inhibitor of the myosin light chain kinase (MLCK) could inhibit EBOV GPΔMuc-dependent viral entry, whereas blebbistatin, a class II myosin ATPase inhibitor, could not. While phosphorylation of myosin II A and B (by MLCK) is required for association with actin and/or plasma membrane, ATPase activity of class II myosins can provide contractile activities for closure of macropinosomes (Mercer and Helenius, 2009; Mercer et al., 2010). We speculate that the contractile activities of other classes of myosins might have a role in macropinosome closure in Vero cells or that myosin II could have an unidentified role in EBOV uptake. Recently, phosphorylated myosin IIA (by MLCK) has been shown to serve as a receptor for gB in mediating HSV-1 entry in Vero cells (Arii et al., 2010). It will therefore be of interest to determine the specific role of class II myosins in EBOV entry.

Role of Pak-1 and Arf6 in EBOV entry

Pak-1 (p21 activated kinase) has been shown to be required during all stages of macropinocytosis (induction, closure and trafficking) (Mercer and Helenius, 2009). Pak-1 is an important regulator of EBOV macropinocytosis since expression of Pak-1AID mutant as well as knockdown of Pak-1 can inhibit EBOV infection (Nanbo et al., 2010; Saeed et al., 2010). Our results (figure 5A-B) have shown that the mucin-like domain has no role in influencing EBOV uptake by Pak-1 dependent macropinocytosis.

Arf6 is a GTPase that aids in recycling Rac1 to the plasma membrane and induces membrane curvature. Arf6 also has a role in plasma membrane remodeling and endocytic membrane trafficking that is independent of Pak-1 (Donaldson, 2003; Mercer and Helenius, 2009). We found that though dominant negative Arf6 (T27N) reduced uptake of dextran, it had little or no effect on EBOV GPΔMuc-dependent entry (figure 5C-D). These results indicate that macropinocytic uptake of EBOV GPΔMuc primarily occurs via a Pak-1 dependent pathway and deletion of the mucin-like domain does not target it to an Arf6 uptake pathway.

Role of Dynamin-2 in EBOV entry

Most viruses that use macropinocytosis (e.g., vaccinia virus, adenovirus serotype3, coxsackievirus B) for entry do not require the large GTPase dynamin-2 for macropinosome closure. Instead, they appear to use CtBP1 for this purpose (Mercer and Helenius, 2009). EBOV entry by macropinocytosis was shown to be dependent on dynamin-2 in SNB19 cells but not in Vero cells (Nanbo et al., 2010; Saeed et al., 2010) (Hunt et al., 2011). Because the receptor tyrosine kinase Axl plays a role in macropinocytic uptake of virus into SNB19 cells but not Vero cells, it seemed possible that the use of dynamin-2 and Axl by EBOV GP is linked. However, in our hands, both pharmacological and genetic approaches reveal a dynamin-2 requirement for EBOV GP-mediated, Axl-independent, entry into Vero cells (figures 6,7). This requirement is determined by the viral glycoprotein and not by the nature or morphology of the viral core (figure 6). Interestingly, the flow cytometry assay for uptake showed that dynasore treatment had no effect on binding as well as uptake, suggesting that EBOV VLPs cannot be stripped from dynasore-treated cells with acid buffer and are likely in membrane-bound vesicles associated with the cell membrane (figure 6E-F). The specific step at which dynamin-2 mediates EBOV entry remains to be determined, but may involve one or more functions of this protein, including its control of Rac1 localization, actomyosin contractile activity, closure of circular ruffles, and trafficking of macropinosomes, (Conner and Schmid, 2003; Mercer and Helenius, 2009).

Our results are in contention with two publications (Nanbo et al., 2010; Saeed et al., 2010) that concluded a dispensable role for dynamin-2 in EBOV macropinocytic uptake and entry. The reason for this discrepancy is unclear at present, but may relate to differences in the dynasore treatment conditions employed in each study. Additionally, while our experiments were performed with a GFP-dynamin-2-K44A enriched population of Vero cells generated by flow sorting, Saeed et al., 2010 used a more heterogenous population of transiently transfected HEK 293T cells in which dynamin-2 inhibition might have been less complete.

We also show that inhibition of dynamin-2 reduces EBOV GP-dependent infection in a mouse dendritic cell line and human adherent PBMCs (figure 8). Although dynamin-2 function is believed to be dispensable for most macropinocytic pathways, some reports have indicated a role for dynamin-2 in PDGF-stimulated and circular ruffle-mediated macropinocytosis (Liu et al., 2008; Mercer and Helenius, 2009; Schlunck et al., 2004). Recently, HIV entry in macrophages was shown to be restricted by dynasore treatment (characteristic of non-classical macropinocytosis) and entry of EBOV in Axl-dependent cells was also inhibited by both dynasore and expression of dynamin-2-K44A (Carter et al., 2011; Hunt et al., 2011).

Concluding remarks

In summary, when expressed on a VSV core or in EBOV VLPs, EBOV GP is sufficient to activate a macropinocytosis-like entry pathway in Vero cells (present study) (Nanbo et al., 2010; Saeed et al., 2010). However, EBOV GP when expressed on lentiviral cores, can enter cells by clathrin-mediated endocytosis (Bhattacharyya et al., 2010; Hunt et al., 2011; Sanchez, 2007). In addition, in certain Axl-dependent cell types, multiple endocytic pathways including macropinocytosis, CME and caveolin-mediated endocytosis may be involved (Hunt et al., 2011). Our studies performed in the Axl-independent Vero cell line indicate that at least in this cell type, EBOV entry occurs predominantly via an atypical macropinocytic pathway. Our findings in adherent human PBMCs and the Jaws mouse dendritic cell line support a role for a similar entry pathway in these antigen-presenting cell types as well.

Taken together, our results demonstrate that entry of EBOV occurs via a non-classical macropinocytic pathway in Vero cells, and indicate that deletion of the mucin-like domain of EBOV GP does not favor entry by other modes of endocytosis such as CME. This mechanism requires an active acto-myosin network and Pak1 activity and is independent of Arf6. However, unlike most macropinocytic pathways, the EBOV entry pathway appears to require the activity of the large GTPase dynamin-2.

Materials and methods

Cells and culture conditions

Vero cells (African green monkey kidney cell line), 293T cells and Jaws (mouse dendritic cell line, a gift from Dr Laura Santambrogio, Albert Einstein College of Medicine) were cultured in high-glucose Dulbecco's modified Eagle's medium containing L-glutamine (DMEM, Invitrogen, Carlsbad, CA) supplemented with 10% fetal bovine serum (Gemini Bioproducts) and 1% penicillin-streptomycin solution (Invitrogen, Carlsbad, CA). Cells were maintained at 37°C in a humidified atmosphere with 5% CO_2.

Plasmid Constructs

The pCAGGS-eGFP-VP40 construct has been described previously (Martin-Serrano et al., 2004). The pCAGGS-RFP-VP40 and pCAGGS-βLaM-VP40 plasmids were constructed by replacing the eGFP cassette by RFP and β-lactamase (βLaM) respectively. The RFP cassette from pRFP vector was amplified by PCR and digested with *Eco*RI and ligated to *Eco*RI digested pCAGGS-eGFP-VP40. Similarly, the βLaM cassette was PCR amplified and cloned into the *Eco*RI digested pCAGGS-eGFP-VP40. The Pak1 wt and Pak1-L107E-83-149 were kindly provided by Dr. Jonathan Chernoff (Fox Chase Cancer Center, PA). The Pak1AID (83-149) was obtained from Addgene (Cambridge, MA). The Arf6 constructs were kindly provided by Dr. Julie G Donaldson (NHLBI, Bethesda, MD). The dynamin constructs were a gift from Dr. Marcelo Ehrlich (Tel Aviv University, Israel).

Reagents and Antibodies

Dynasore was purchased from Sigma-Aldrich, St. Louis, MO. EIPA, ML9, Blebbistatin, LatA and rottlerin were purchased from Enzo Life Sciences, Plymouth Meeting, PA. Anti-Dynamin-2 antibody C-18 was purchased from Santa Cruz Biotechnology, CA. Anti-L antibody for VSV-L protein has been described (Heinrich et al., 2010). Secondary antibodies (anti-goat-Alexa-594, anti-rabbit-Alexa-488) were purchased from Jackson ImmunoResearch Laboratories, Inc., PA. WGA-rhodamine was from Vector laboratories (Burlingame, CA) and WGA-Alexa647 was from Molecular Probes (Carlsbad, CA). Transferrin-Alexa-647 and FITC-dextran MW10K were from Molecular probes, CA and Sigma-Aldrich, MO respectively.

Virus preparation

rVSV-GPΔMuc (deleted mucin domain), rVSV-GP-FL (full length), rVSV-G were amplified in Vero cells, concentrated by pelleting through 10% sucrose cushions prepared in NT (10 mM Tris.Cl pH[7.4], 135 mM NaCl), resuspended in NT, and stored at -80°C. These concentrated virus preparations routinely contained infectious titers of ~1×10^{10} infectious units per mL. All experiments with rVSV-GP were carried out using enhanced biosafety level 2 procedures approved by the Einstein Institutional Biosafety Committee (Wong et al., 2010). VSV pseudotypes expressing eGFP and bearing VSV G (VSV-G) or EBOV GPΔMuc (VSV-GPΔMuc) were generated as described previously (Chandran et al., 2005).

VLP production

293T cells plated onto 150mm plates were co-transfected (1:1) with pCAGGS vector expressing GPΔMuc (15 μg) and N-terminal fusion of βLaM-VP40 (15 μg) using Lipofectamine 2000 (Invitrogen, Carlsbad, CA) per the manufacturer's instructions. No antibiotics were used in the culture medium. 18 hours post-transfection, the medium was changed and the supernatant was collected after another 48 hours. The βLaM-VLPs were pelleted by ultracentrifugation at 25,000 rpm. The VLPs were next purified in a 10% sucrose cushion by ultracentrifugation at 40,000 rpm and resuspended in PBS and frozen (-80°C) as aliquots. The same protocol was followed for production of eGFP-VLPs, RFP-fused VLPs, and βLaM-VLPs bearing EBOV GP-FL.

Inhibitor treatment

Vero cells were pre-treated with 1% DMSO, EIPA (25 μM), latrunculin A (0.01 μM), rottlerin (2.5 μM), ML9 (5 μM) or 50 μM blebbistatin for 1 hour in serum-containing medium. Cells were infected with rVSVs expressing the VSV-G protein or EBOV GP. Viral entry was allowed to occur for 1 hour in the presence of drugs and then further infection was inhibited by incubating cells with medium containing 20 mM ammonium chloride. Infection was scored the next day by counting eGFP-positive cells.

Dynasore treatment

Vero cells (70% confluent) plated in serum-containing medium were washed several times with PBS. Cells were then incubated at 37°C in serum-free medium containing dynasore for 30 min (Kirchhausen et al., 2008). Virus or VLP infection was carried out and infection was allowed to occur in dynasore containing serum-free medium for the indicated time points for VLPs at 37°C. VSV pseudotype and rVSV infection was allowed to occur for 1 hour at 37°C followed by inhibition of further entry in the presence of medium containing 20 mM ammonium chloride.

βLaM-VLP assay for entry

Vero cells (2.5×10^5) were plated onto 12-well plates sixteen hours before infection in antibiotic-free medium. The cells were then treated with indicated drugs for 1 hour and with E-64 (300 μM) 2 hours before infection. Control wells were treated with medium containing 1% DMSO respectively. The treated cells were spin-inoculated with βLaM-VLPs at 2500 rpm for 10 min at 4°C and then incubated for 60 min at 37°C in the presence of medium containing drugs to allow entry. Cells were then trypsinized and labeled with CCF2-AM (Invitrogen, Carlsbad, CA) per the manufacturer's instructions in the presence of 20 mM ammonium chloride to inhibit any further infection. Briefly, cells were loaded with 1X loading solution of CCF2-AM containing 20 mM ammonium chloride for 1 hour at room temperature. The cells were then washed and incubated overnight in CO_2 independent medium (containing 20 mM ammonium chloride and 2.5 mM probenecid) at room temperature to allow the βLaM enzymatic reaction to occur (Martinez et al., 2010; Yonezawa et al., 2005). Finally, cells were washed with PBS and fixed in 1.2% formaldehyde solution for flow cytometry analysis. The change in emission fluorescence of CCF2 (520nm to 427nm) post cleavage by βLaM-VP40 was analyzed by the BD-LSRII (Becton-Dickinson, San Jose, CA). Live cells were analyzed based on forward scatter and data analysis was done using Win-MDI.

VLP binding and uptake assay (flow cytometry)

Vero cells, treated with drugs or 1% DMSO, were spin-inoculated with eGFP-VLPs at 4°C for 10 min. To determine the percentage of bound VLPs, cells were washed once with cold PBS, scraped in cold PBS with 2% FBS and then assayed for GFP fluorescence by flow

cytometry. For uptake, spin-inoculated cells were incubated in the presence of drugs for 30 min at 37°C. Un-internalized VLPs were stripped off these cells by incubating in acid wash buffer for 2 min. Cells were then washed with cold PBS and then harvested by trypsin treatment and assayed for GFP fluorescence in cold PBS with 2% FBS by flow cytometry. The BD-FACS Calibur was used for flow cytometry. In the case of thirty-six hour transfected Vero cells, cells were spin-inoculated as described above and uptake was assayed in double GFP-RFP positive cells.

Plasmid transfection and infection assay

Vero cells (1×10^6) were transfected using Lipofectamine 2000 (according to the manufacturer's protocol, Invitrogen, CA) with the indicated plasmid constructs. Thirty-six hours post-transfection, cells were infected with VSV-G or VSV-GP luciferase viruses. The infection was allowed to occur for 16 hours. GFP positive cells (300,000) were then sorted using the FACS Aria and assayed for luciferase activity to determine infection. Luciferase activity was assayed using Steady Glo (Promega, WI).

Dextran uptake assay

Vero cells were serum-starved for 2 hours and then treated with 1% DMSO (control), 25 μM EIPA or 10 nM PMA for 1 hour at 37°C. The cells were then pulsed with 0.5 mg/mL FITC-labeled dextran (10K Mw) for the indicated time points at 37°C in the presence of drugs. Unbound dextran was stripped off the cells by trypsin treatment and percent uptake was determined by flow cytometry.

Transferrin uptake assay

Vero cells were washed with PBS and then incubated in serum-free medium for 2 hours. Cells were treated with 1% DMSO or dynasore for 30 min and then pulsed with 1 μg/mL Alexa-647-labeled transferrin for the indicated time points. Thirty-six hour transfected cells were incubated in serum-free medium for 2 hours and pulsed with 1 μg/mL Alexa-647-labeled transferrin for the indicated time points. Cells were harvested by acid washing for 2 min followed by trypsin treatment and harvested in cold PBS with 2% FBS. Transferrin internalization was assayed by flow cytometry using the BD-FACS Calibur.

Immunofluorescence staining

Cells were fixed in 2% PFA for 30 min at room temperature and washed with PBS. Next the cells were incubated in 0.1M glycine buffer for 10 min and then washed with PBS. Cell were then permeabilized in PBS-0.1%BSA- 0.1% Triton X for 1 hour and stained with the respective primary antibodies for 2 hours at room temperature. Next, cells were washed and stained with the respective secondary antibodies (1:500). For wheat germ agglutinin (WGA) staining, fixed cells were incubated in 0.1M glycine buffer for 10 min, washed with PBS and stained with WGA in PBS (1:2000) for 2 min followed by washing in PBS and then mounting on to slides with Prolong Gold (Molecular probes, CA).

Confocal Microscopy

Cover slips were mounted onto slides with Prolong gold (Molecular probes, CA). Cells were imaged using a 60X oil immersion objective on the Leica TCS SP2 AOBS confocal microscope (Mannheim, Germany) in the Analytical Imaging Facility at Einstein: College of Medicine. Detection ranges were set to eliminate crosstalk between fluorophores. Cells were randomly selected for imaging and z series of all images were taken. Images were processed using Image J software and maximal z projections of mid-sections are shown. The results are representative of 3 different experiments. The colocalization plug-in in Image J was used

to shown merge of two colors and also the colocalized points. The JaCop plug-in in Image J was used to determine the Pearson's coefficient for colocalization.

Electron Microscopy

Confluent Vero cell monolayers were inoculated with rVSV expressing EBOV GP at a MOI of 200 for 15 min, 30 min and 3 hours. Subsequently, cells were fixed for 1 hour at room temperature in a mixture of 2.5% glutaraldehyde, 1.25% paraformaldehyde and 0.03% picric acid in 0.1M sodium cacodylate buffer (pH 7.4). Samples were washed extensively in 0.1M sodium cacodylate buffer (pH 7.4) after which they were treated with 1% osmium tetroxide and 1.5% potassium ferrocyanide in water for 30 min at room temperature. Treated samples were washed in water, stained in 1% aqueous uranyl acetate for 30 min, and dehydrated in grades of alcohol (70%, 90%, 2×100%) for 5 min each. Cells were removed from the culture dish with propyleneoxide and pelleted at 3,000 rpm for 3 min. Samples were infiltrated with Epon mixed with propyleneoxide (1:1) for 2 hours at room temperature. Samples were embedded in fresh Epon and left to polymerize for 48 hours at 65°C. Ultrathin sections (about 60–80 nm) were cut on a Reichert Ultracut-S microtome and placed onto copper grids. Images were acquired using a Technai G^2 Spirit BioTWIN (Fei, Hillsboro, OR) transmission electron microscope. Images were processed using Adobe Photoshop CS4.

PBMC infection assay

PBMCs were isolated from human peripheral blood by Ficoll Hypaque centrifugation. CD14 positive cells were purified using CD14 magnetic beads (Miltenyi Biotec, Germany). CD14 positive PBMCs (2×10^6) were allowed to differentiate in 48-well plates and RPMI medium supplemented with 10% FCS and GMCSF for 5 days. Cells were then treated with 0.5% DMSO, 60 μM Dynasore, 25 μM EIPA and 300 μM E-64d for 1 hour, following which cells were infected with rVSVs expressing VSV-G, EBOV GPΔMuc and EBOV GP-FL for 24 hours at 37°C. Supernatant from infected cells was collected and tittered onto Vero cells as described earlier.

Supplementary Material

Refer to Web version on PubMed Central for supplementary material.

Acknowledgments

We thank M.C. Kielian and A. Krishnan for their feedback on preliminary versions of this manuscript. We are grateful to G. Bricard and S.A. Porcelli for help with the human PBMCs. We also acknowledge Frank Macaluso, Vera DesMarais, Leslie Gunther and Christina Polumbo at the Einstein Analytical Imaging Facility. This work was supported by the National Institutes of Health (NIH) grants R01 AI088027 (to K.C.), R01 AI081842 (to S.P.W), R01 AI047140-06 (to J.C.T) and by the NERCE (New England Regional Center of Excellence) grant AI057159 (to S.P.W.).

References

1. Alvarez CP, Lasala F, Carrillo J, Muniz O, Corbi AL, Delgado R. C-type lectins DC-SIGN and L-SIGN mediate cellular entry by Ebola virus in cis and in trans. J Virol. 2002; 76:6841–6844. [PubMed: 12050398]
2. Arii J, Goto H, Suenaga T, Oyama M, Kozuka-Hata H, Imai T, Minowa A, Akashi H, Arase H, Kawaoka Y, Kawaguchi Y. Non-muscle myosin IIA is a functional entry receptor for herpes simplex virus-1. Nature. 2010; 467:859–862. [PubMed: 20944748]
3. Ascenzi P, Bocedi A, Heptonstall J, Capobianchi MR, Di Caro A, Mastrangelo E, Bolognesi M, Ippolito G. Ebolavirus and Marburgvirus: insight the Filoviridae family. Mol Aspects Med. 2008; 29:151–185. [PubMed: 18063023]

4. Bhattacharyya S, Warfield KL, Ruthel G, Bavari S, Aman MJ, Hope TJ. Ebola virus uses clathrin-mediated endocytosis as an entry pathway. Virology. 2010; 401:18–28. [PubMed: 20202662]
5. Bray M, Geisbert TW. Ebola virus: the role of macrophages and dendritic cells in the pathogenesis of Ebola hemorrhagic fever. Int J Biochem Cell Biol. 2005; 37:1560–1566. [PubMed: 15896665]
6. Brindley MA, Hunt CL, Kondratowicz AS, Bowman J, Sinn PL, McCray PB Jr. Quinn K, Weller ML, Chiorini JA, Maury W. Tyrosine kinase receptor Axl enhances entry of Zaire ebolavirus without direct interactions with the viral glycoprotein. Virology. 2011
7. Carter GC, Bernstone L, Baskaran D, James W. HIV-1 infects macrophages by exploiting an endocytic route dependent on dynamin, Rac1 and Pak1. Virology. 2011; 409:234–250. [PubMed: 21056892]
8. Chan SY, Empig CJ, Welte FJ, Speck RF, Schmaljohn A, Kreisberg JF, Goldsmith MA. Folate receptor-alpha is a cofactor for cellular entry by Marburg and Ebola viruses. Cell. 2001; 106:117–126. [PubMed: 11461707]
9. Chandran K, Sullivan NJ, Felbor U, Whelan SP, Cunningham JM. Endosomal proteolysis of the Ebola virus glycoprotein is necessary for infection. Science. 2005; 308:1643–1645. [PubMed: 15831716]
10. Conner SD, Schmid SL. Regulated portals of entry into the cell. Nature. 2003; 422:37–44. [PubMed: 12621426]
11. Donaldson JG. Multiple roles for Arf6: sorting, structuring, and signaling at the plasma membrane. J Biol Chem. 2003; 278:41573–41576. [PubMed: 12912991]
12. Feldmann H, Geisbert T, Kawaoka Y. Filoviruses: recent advances and future challenges. J Infect Dis 196 Suppl. 2007; 2:S129–130.
13. Geisbert TW, Hensley LE, Larsen T, Young HA, Reed DS, Geisbert JB, Scott DP, Kagan E, Jahrling PB, Davis KJ. Pathogenesis of Ebola hemorrhagic fever in cynomolgus macaques: evidence that dendritic cells are early and sustained targets of infection. Am J Pathol. 2003; 163:2347–2370. [PubMed: 14633608]
14. Heinrich BS, Cureton DK, Rahmeh AA, Whelan SP. Protein expression redirects vesicular stomatitis virus RNA synthesis to cytoplasmic inclusions. PLoS Pathog. 2010; 6:e1000958. [PubMed: 20585632]
15. Hewlett LJ, Prescott AR, Watts C. The coated pit and macropinocytic pathways serve distinct endosome populations. J Cell Biol. 1994; 124:689–703. [PubMed: 8120092]
16. Hunt CL, Kolokoltsov AA, Davey RA, Maury W. The Tyro3 receptor kinase Axl enhances macropinocytosis of Zaire ebolavirus. J Virol. 2011; 85:334–347. [PubMed: 21047970]
17. Ji X, Olinger GG, Aris S, Chen Y, Gewurz H, Spear GT. Mannose-binding lectin binds to Ebola and Marburg envelope glycoproteins, resulting in blocking of virus interaction with DC-SIGN and complement-mediated virus neutralization. J Gen Virol. 2005; 86:2535–2542. [PubMed: 16099912]
18. Kirchhausen T, Macia E, Pelish HE. Use of dynasore, the small molecule inhibitor of dynamin, in the regulation of endocytosis. Methods Enzymol. 2008; 438:77–93. [PubMed: 18413242]
19. Koivusalo M, Welch C, Hayashi H, Scott CC, Kim M, Alexander T, Touret N, Hahn KM, Grinstein S. Amiloride inhibits macropinocytosis by lowering submembranous pH and preventing Rac1 and Cdc42 signaling. J Cell Biol. 2010; 188:547–563. [PubMed: 20156964]
20. Kondratowicz AS, Lennemann NJ, Sinn PL, Davey RA, Hunt CL, Moller-Tank S, Meyerholz DK, Rennert P, Mullins RF, Brindley M, Sandersfeld LM, Quinn K, Weller M, McCray PB Jr. Chiorini J, Maury W. T-cell immunoglobulin and mucin domain 1 (TIM-1) is a receptor for Zaire Ebolavirus and Lake Victoria Marburgvirus. Proc Natl Acad Sci U S A. 2011
21. Kuhn JH. Filoviruses. A compendium of 40 years of epidemiological, clinical, and laboratory studies. Arch Virol Suppl. 2008; 20:13–360. [PubMed: 18637412]
22. Kuhn JH, Becker S, Ebihara H, Geisbert TW, Johnson KM, Kawaoka Y, Lipkin WI, Negredo AI, Netesov SV, Nichol ST, Palacios G, Peters CJ, Tenorio A, Volchkov VE, Jahrling PB. Proposal for a revised taxonomy of the family Filoviridae: classification, names of taxa and viruses, and virus abbreviations. Arch Virol. 2010; 155:2083–2103. [PubMed: 21046175]

23. Lee JE, Fusco ML, Hessell AJ, Oswald WB, Burton DR, Saphire EO. Structure of the Ebola virus glycoprotein bound to an antibody from a human survivor. Nature. 2008; 454:177–182. [PubMed: 18615077]
24. Lee JE, Saphire EO. Neutralizing ebolavirus: structural insights into the envelope glycoprotein and antibodies targeted against it. Curr Opin Struct Biol. 2009; 19:408–417. [PubMed: 19559599]
25. Liberali P, Kakkonen E, Turacchio G, Valente C, Spaar A, Perinetti G, Bockmann RA, Corda D, Colanzi A, Marjomaki V, Luini A. The closure of Pak1-dependent macropinosomes requires the phosphorylation of CtBP1/BARS. Embo J. 2008; 27:970–981. [PubMed: 18354494]
26. Lin G, Simmons G, Pohlmann S, Baribaud F, Ni H, Leslie GJ, Haggarty BS, Bates P, Weissman D, Hoxie JA, Doms RW. Differential N-linked glycosylation of human immunodeficiency virus and Ebola virus envelope glycoproteins modulates interactions with DC-SIGN and DC-SIGNR. J Virol. 2003; 77:1337–1346. [PubMed: 12502850]
27. Liu YW, Surka MC, Schroeter T, Lukiyanchuk V, Schmid SL. Isoform and splice-variant specific functions of dynamin-2 revealed by analysis of conditional knock-out cells. Mol Biol Cell. 2008; 19:5347–5359. [PubMed: 18923138]
28. Martin-Serrano J, Perez-Caballero D, Bieniasz PD. Context-dependent effects of L domains and ubiquitination on viral budding. J Virol. 2004; 78:5554–5563. [PubMed: 15140952]
29. Martinez O, Johnson J, Manicassamy B, Rong L, Olinger GG, Hensley LE, Basler CF. Zaire Ebola virus entry into human dendritic cells is insensitive to cathepsin L inhibition. Cell Microbiol. 2010; 12:148–157. [PubMed: 19775255]
30. Mercer J, Helenius A. Virus entry by macropinocytosis. Nat Cell Biol. 2009; 11:510–520. [PubMed: 19404330]
31. Mercer J, Schelhaas M, Helenius A. Virus entry by endocytosis. Annu Rev Biochem. 2010; 79:803–833. [PubMed: 20196649]
32. Nanbo A, Imai M, Watanabe S, Noda T, Takahashi K, Neumann G, Halfmann P, Kawaoka Y. Ebolavirus is internalized into host cells via macropinocytosis in a viral glycoprotein-dependent manner. PLoS Pathog 6. 2010
33. Ohtsubo K, Marth JD. Glycosylation in cellular mechanisms of health and disease. Cell. 2006; 126:855–867. [PubMed: 16959566]
34. Quinn K, Brindley MA, Weller ML, Kaludov N, Kondratowicz A, Hunt CL, Sinn PL, McCray PB Jr. Stein CS, Davidson BL, Flick R, Mandell R, Staplin W, Maury W, Chiorini JA. Rho GTPases modulate entry of Ebola virus and vesicular stomatitis virus pseudotyped vectors. J Virol. 2009; 83:10176–10186. [PubMed: 19625394]
35. Quirin K, Eschli B, Scheu I, Poort L, Kartenbeck J, Helenius A. Lymphocytic choriomeningitis virus uses a novel endocytic pathway for infectious entry via late endosomes. Virology. 2008; 378:21–33. [PubMed: 18554681]
36. Saeed MF, Kolokoltsov AA, Albrecht T, Davey RA. Cellular entry of ebola virus involves uptake by a macropinocytosis-like mechanism and subsequent trafficking through early and late endosomes. PLoS Pathog. 2010; 6
37. Sanchez A. Analysis of filovirus entry into vero e6 cells, using inhibitors of endocytosis, endosomal acidification, structural integrity, and cathepsin (B and L) activity. J Infect Dis. 2007; 196(Suppl 2):S251–258. [PubMed: 17940957]
38. Schlunck G, Damke H, Kiosses WB, Rusk N, Symons MH, Waterman-Storer CM, Schmid SL, Schwartz MA. Modulation of Rac localization and function by dynamin. Mol Biol Cell. 2004; 15:256–267. [PubMed: 14617821]
39. Schornberg K, Matsuyama S, Kabsch K, Delos S, Bouton A, White J. Role of endosomal cathepsins in entry mediated by the Ebola virus glycoprotein. J Virol. 2006; 80:4174–4178. [PubMed: 16571833]
40. Simmons G, Reeves JD, Grogan CC, Vandenberghe LH, Baribaud F, Whitbeck JC, Burke E, Buchmeier MJ, Soilleux EJ, Riley JL, Doms RW, Bates P, Pohlmann S. DC-SIGN and DC-SIGNR bind ebola glycoproteins and enhance infection of macrophages and endothelial cells. Virology. 2003a; 305:115–123. [PubMed: 12504546]

41. Simmons G, Rennekamp AJ, Chai N, Vandenberghe LH, Riley JL, Bates P. Folate receptor alpha and caveolae are not required for Ebola virus glycoprotein-mediated viral infection. J Virol. 2003b; 77:13433–13438. [PubMed: 14645601]

42. Simmons G, Wool-Lewis RJ, Baribaud F, Netter RC, Bates P. Ebola virus glycoproteins induce global surface protein down-modulation and loss of cell adherence. J Virol. 2002; 76:2518–2528. [PubMed: 11836430]

43. Takada A, Fujioka K, Tsuiji M, Morikawa A, Higashi N, Ebihara H, Kobasa D, Feldmann H, Irimura T, Kawaoka Y. Human macrophage C-type lectin specific for galactose and N-acetylgalactosamine promotes filovirus entry. J Virol. 2004; 78:2943–2947. [PubMed: 14990712]

44. Takada A, Robison C, Goto H, Sanchez A, Murti KG, Whitt MA, Kawaoka Y. A system for functional analysis of Ebola virus glycoprotein. Proc Natl Acad Sci U S A. 1997; 94:14764–14769. [PubMed: 9405687]

45. Takada A, Watanabe S, Ito H, Okazaki K, Kida H, Kawaoka Y. Downregulation of beta1 integrins by Ebola virus glycoprotein: implication for virus entry. Virology. 2000; 278:20–26. [PubMed: 11112476]

46. Wilson JA, Hevey M, Bakken R, Guest S, Bray M, Schmaljohn AL, Hart MK. Epitopes involved in antibody-mediated protection from Ebola virus. Science. 2000; 287:1664–1666. [PubMed: 10698744]

47. Wong AC, Sandesara RG, Mulherkar N, Whelan SP, Chandran K. A forward genetic strategy reveals destabilizing mutations in the Ebolavirus glycoprotein that alter its protease dependence during cell entry. J Virol. 2010; 84:163–175. [PubMed: 19846533]

48. Wool-Lewis RJ, Bates P. Characterization of Ebola virus entry by using pseudotyped viruses: identification of receptor-deficient cell lines. J Virol. 1998; 72:3155–3160. [PubMed: 9525641]

49. Yonezawa A, Cavrois M, Greene WC. Studies of ebola virus glycoprotein-mediated entry and fusion by using pseudotyped human immunodeficiency virus type 1 virions: involvement of cytoskeletal proteins and enhancement by tumor necrosis factor alpha. J Virol. 2005; 79:918–926. [PubMed: 15613320]

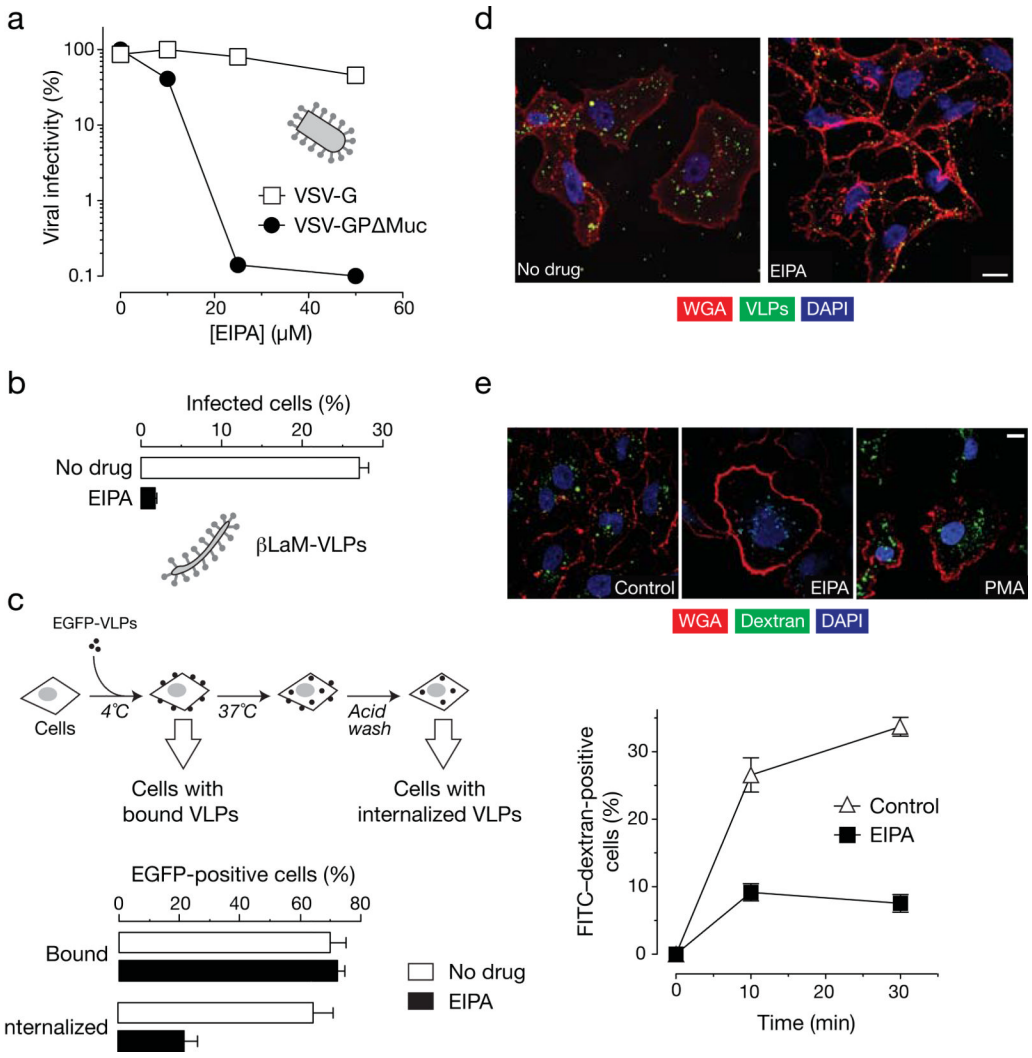

Figure 1. Macropinocytosis inhibitor EIPA inhibits EBOV GPΔMuc-dependent infection by inhibiting uptake

(A) EIPA inhibits infection by VSV-GPΔMuc but not VSV-G. Vero cells were pre-treated with the indicated concentrations of the macropinocytosis inhibitor EIPA and exposed to virus. (B) EIPA inhibits infection of EBOV VLPs. Vero cells were pre-treated with the indicated inhibitors and then exposed to β-lactamase-fused EBOV VLPs (βLaM-VLPs). VLP entry was measured by quantitation of the percentage of cells containing cleaved CCF2 (positive for blue fluorescence). (C) EIPA does not affect binding but inhibits uptake of EBOV VLPs (flow cytometry). eGFP-fused EBOV VLPs (eGFP-VLPs) were spin-inoculated on to Vero cells pre-treated for 1 hour with 25 μM EIPA or 1% DMSO at 4°C for 10 min. The percentage of bound VLPs was determined by flow cytometry. To allow VLP uptake, cells were shifted to 37°C for 30 min in the presence of drugs. Un-internalized VLPs were stripped off cells by incubation with acid wash buffer for 2 min after which eGFP fluorescence was quantitated by flow cytometry. (D) EIPA inhibits uptake of EBOV VLPs (microscopy). Vero cells were pre- with drug vehicle (1% DMSO) or 25 μM EIPA and then exposed to eGFP-VLPs. Entry was allowed to proceed for 30 min at 37°C. Cells were then fixed and stained with rhodamine-labeled wheat germ agglutinin (WGA) and subjected to confocal microscopy. Representative maximal Z projections of middle slices are shown. Scale bars are 10 μM. (E) 25 μM EIPA inhibits uptake of FITC-dextran. Vero were pulsed

with 0.5 mg/mL FITC-labeled dextran (10K MW) for the indicated time points at 37°C in the presence of drugs. Unbound dextran was stripped off the cells by trypsin treatment and VLP uptake was determined by flow cytometry. Similarly-treated cells on coverslips were fixed at the indicated times and stained with rhodamine-WGA. FITC-dextran uptake was assayed by confocal microscopy. Representative maximal z projections of middle slices of 30 min time points are shown. Scale bars, 10 μM. (A-E) Means +/-SD are shown.

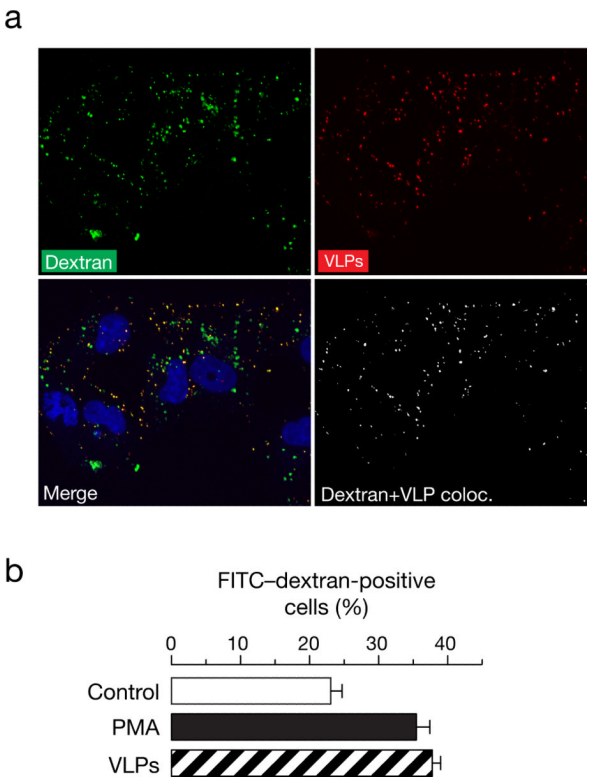

Figure 2. EBOV VLPs colocalize with and induce the uptake of fluid phase uptake markers

(A) EBOV VLPs colocalize with FITC-labeled dextran. Vero cells were spin-inoculated with RFP-labeled EBOV VLPs at 4°C for 10 min and then pulsed with 0.5 mg/mL of FITC-dextran for 10 min at 37°C. The cells were then fixed in 2% PFA and washed. Images shown are representative maximal Z projections of middle slices. Scale bars, 10 μM. (B) EBOV VLPs induce uptake of FITC-dextran. Serum-starved Vero cells were pre-treated with 1% DMSO (control), spin-inoculated EBOV VLPs, or 10nM PMA for 1 hour at 37°C. Uptake of FITC-labeled dextran (10K MW) at 37°C for 30 min was determined by flow cytometry. Means +/-SD of three replicates are shown.

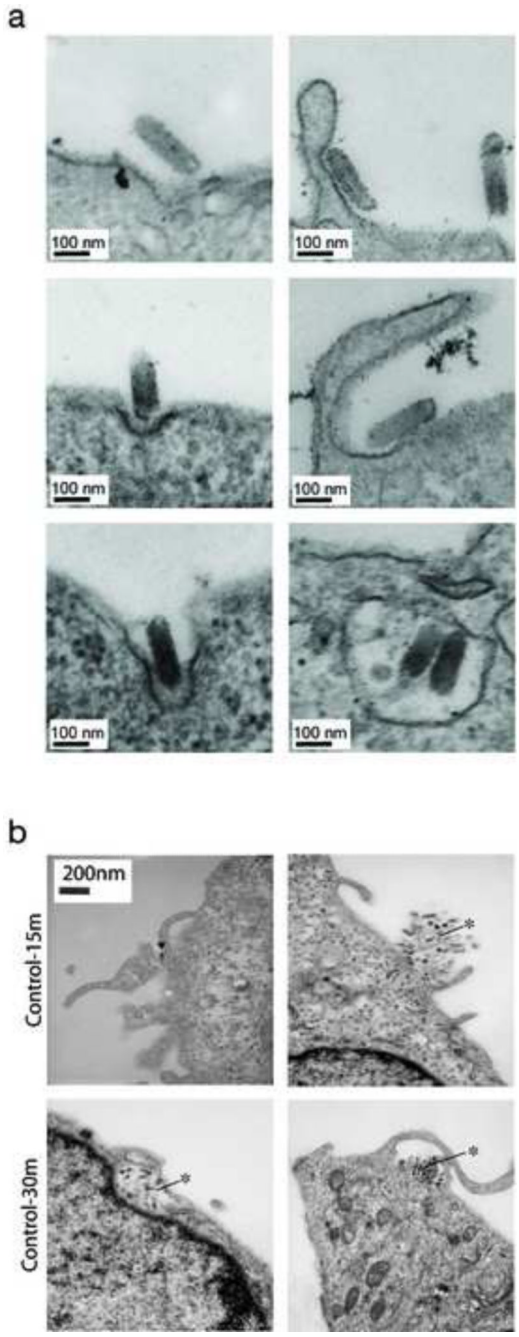

Figure 3. Visualization of EBOV GPΔMuc-dependent viral uptake by transmission electron microscopy

(A) Electron micrographs show entry of rVSV-G into Vero cells via clathrin-coated pits. By contrast, rVSV-GPΔMuc induces membrane ruffling and enters cells by a macropinocytosis-like pathway. These images were taken at 3 hours post-infection. (B) Electron micrographs of Vero cells at 15 and 30 min post-infection. The arrow indicates a single VSV-GPΔMuc particle and the asterisk shows aggregates.

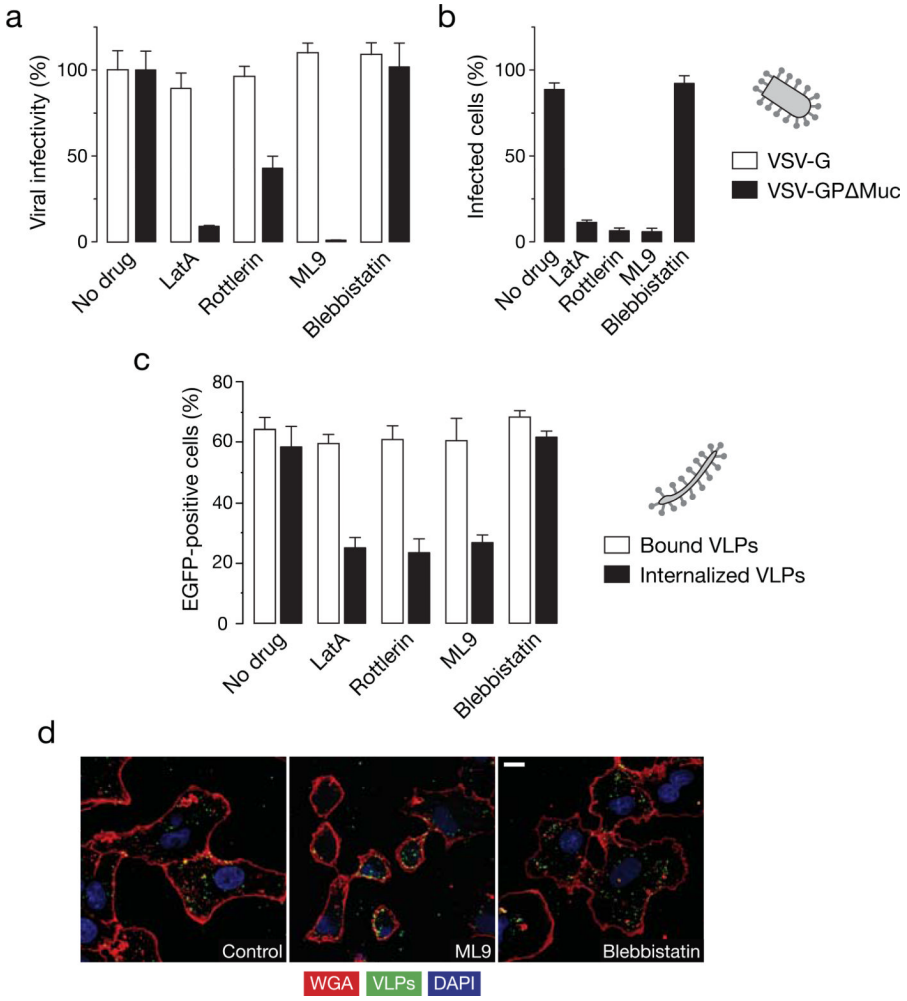

Figure 4. Actin, myosin, and PKC inhibitors can inhibit EBOV GPΔMuc-dependent viral uptake and infection in Vero cells

(A) Inhibitors of PKC and the actomyosin framework inhibit infection by VSV-EBOV GPΔMuc but not VSV-G. Vero cells pre-treated with 1% DMSO, latrunculin A (0.01 μM), rottlerin (2.5 μM), ML9 (5 μM) or 50 μM blebbistatin were exposed to rVSV-GPΔMuc or rVSV-G. Infection was scored the next day by counting eGFP-positive cells. (B) Inhibitors of PKC and the actomyosin framework reduce entry by EBOV VLPs. Entry of βLaM-VLPs into Vero cells pre-treated with the indicated inhibitors was assessed by flow cytometry. Data are normalized to the untreated samples. (C) Latrunculin A, rottlerin, and ML9 inhibit uptake but not binding of EBOV VLPs. VLP binding and internalization was measured by flow cytometry in inhibitor-treated Vero cells. (D) ML9 inhibits uptake of EBOV VLPs, but blebbistatin does not. Representative maximal Z projections of Vero cells pre-treated with inhibitors and exposed to eGFP-VLPs for 30 min are shown. Scale bars, 5 μM. (A-C) Means +/-SD of three replicates are shown.

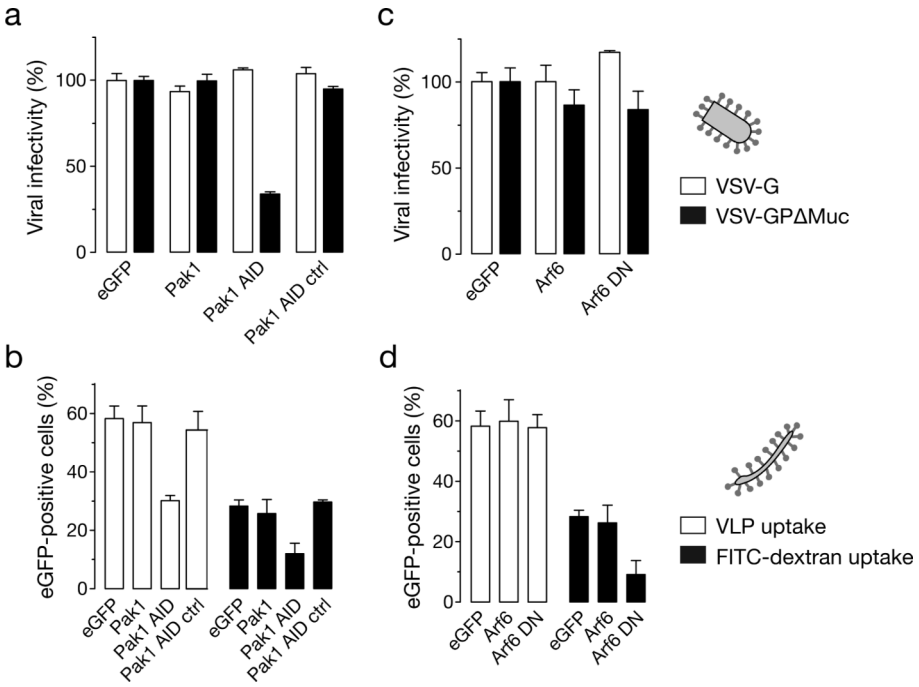

Figure 5. Pak-1 plays an important role in mediating EBOV GPΔMuc-dependent entry into Vero cells

(A) Expression of the Pak-1 autoinhibitory domain (AID) inhibits infection by VSV-GPΔMuc but not VSV-G. Vero cells cotransfected with eGFP and Pak-1 expressing plasmids were exposed to VSV-G or VSV-GPΔMuc expressing firefly luciferase from the viral genome. FACS-sorted eGFP-positive cells were assayed for luciferase activity to quantitate infection. Infection is normalized to the control vector co-transfected with eGFP for both viruses. (B) Pak-1 AID expression inhibits uptake of EBOV VLPs and FITC-dextran. Vero cells co-transfected with RFP and Pak-1 expressing plasmids were assessed for uptake of VLPs and FITC-dextran in RFP positive cells by flow cytometry. Results plotted are a mean+/-SD of three replicates. (C) Expression of an Arf6 dominant-negative mutant has no effect on VSV-GPΔMuc infection. Vero cells cotransfected with eGFP and Arf6-expressing plasmids were exposed to luciferase-expressing VSV-G or VSV-GPΔMuc. Expression of the virus-encoded luciferase in FACS-sorted eGFP-positive cells was quantitated as described in (A). (D) Expression of an Arf6 dominant-negative mutant has no effect on the uptake of EBOV VLPs. Vero cells cotransfected with RFP and Arf6-expressing plasmids were assessed for uptake of VLPs and FITC-dextran as described in (B). (A-D) Means +/-SD of three replicates are shown.

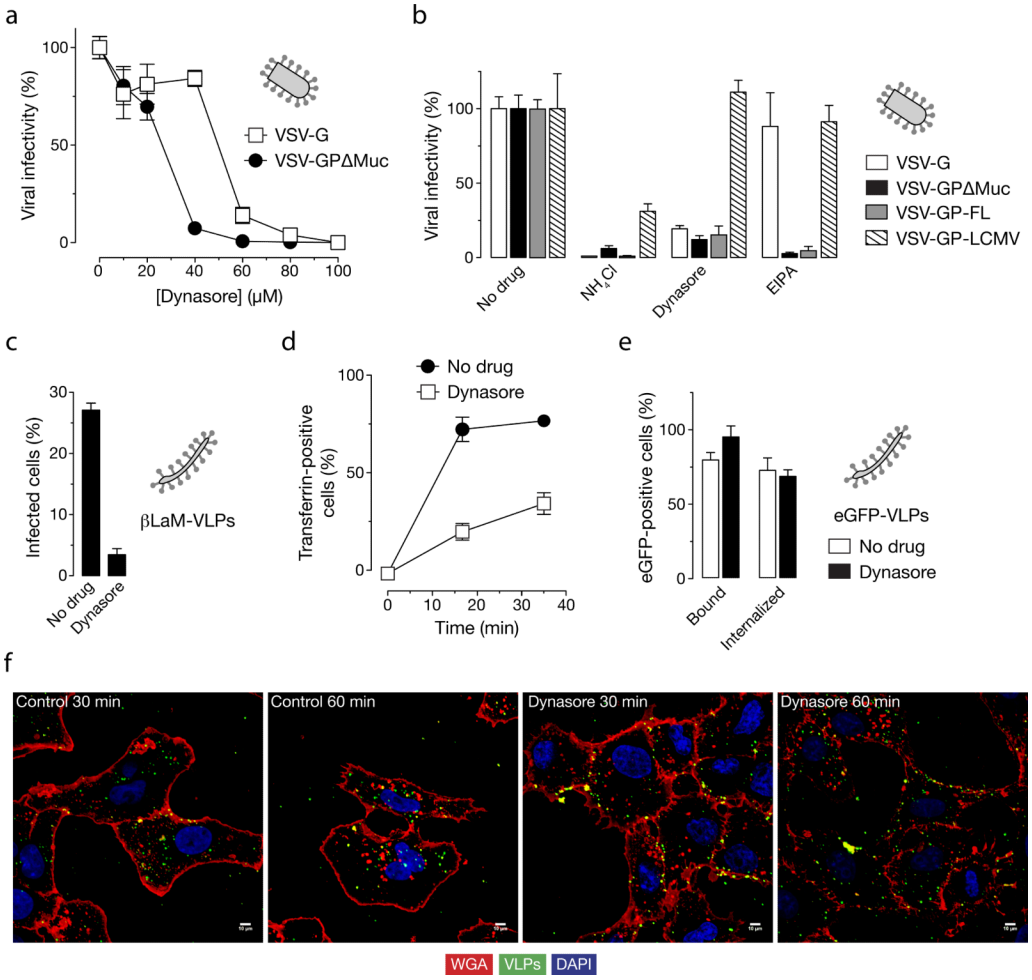

Figure 6. Dynasore reduces EBOV GPΔMuc-dependent infection by inhibiting viral uptake

(A) Dynasore inhibits infection by VSV-GPΔMuc. Vero cells were treated with the indicated concentrations of the dynamin inhibitor dynasore and then exposed to VSV-GPΔMuc or VSV-G. Infection was scored by counting eGFP-positive cells. (B) Dynasore inhibits infection by VSV-GP-FL and VSV-GPΔMuc but not VSV-LCMV GP. Vero cells were pre-treated with 1% DMSO, 120 μM dynasore, 25 μM EIPA or 20 mM ammonium chloride and then exposed to virus. Infection was scored by counting eGFP-positive cells (VSV-GP and VSV-G) or Alexa-488-positive cells after immunostaining for the viral glycoprotein (VSV-LCMV GP). (C) Dynasore inhibits infection of βLaM-VLPs. Entry of βLaM-VLPs into Vero cells pre-treated with dynasore was quantitated by flow cytometry. (D) Dynasore inhibits transferrin uptake. Dynasore-treated cells were pulsed with 1 μg/mL Alexa-647-labeled transferrin for the indicated times, and transferrin internalization was assessed by flow cytometry. (E) Effect of dynasore on VLP uptake (flow cytometry). Dynasore-treated cells were spin-inoculated with eGFP-VLPs and internalization was allowed to occur for 30 min at 37°C. Internalized VLPs were assayed by flow cytometry. (F) Dynasore inhibits uptake of eGFP-VLPs (microscopy). Vero cells pre-treated with dynasore were spin-inoculated with eGFP-VLPs, incubated in the presence of drug at 37°C for the indicated times, and then fixed. Representative maximal Z projections of middle slices from confocal microscopy are shown. Scale bars, 5 μM. (A-E) Means +/-SD of three replicates are shown.

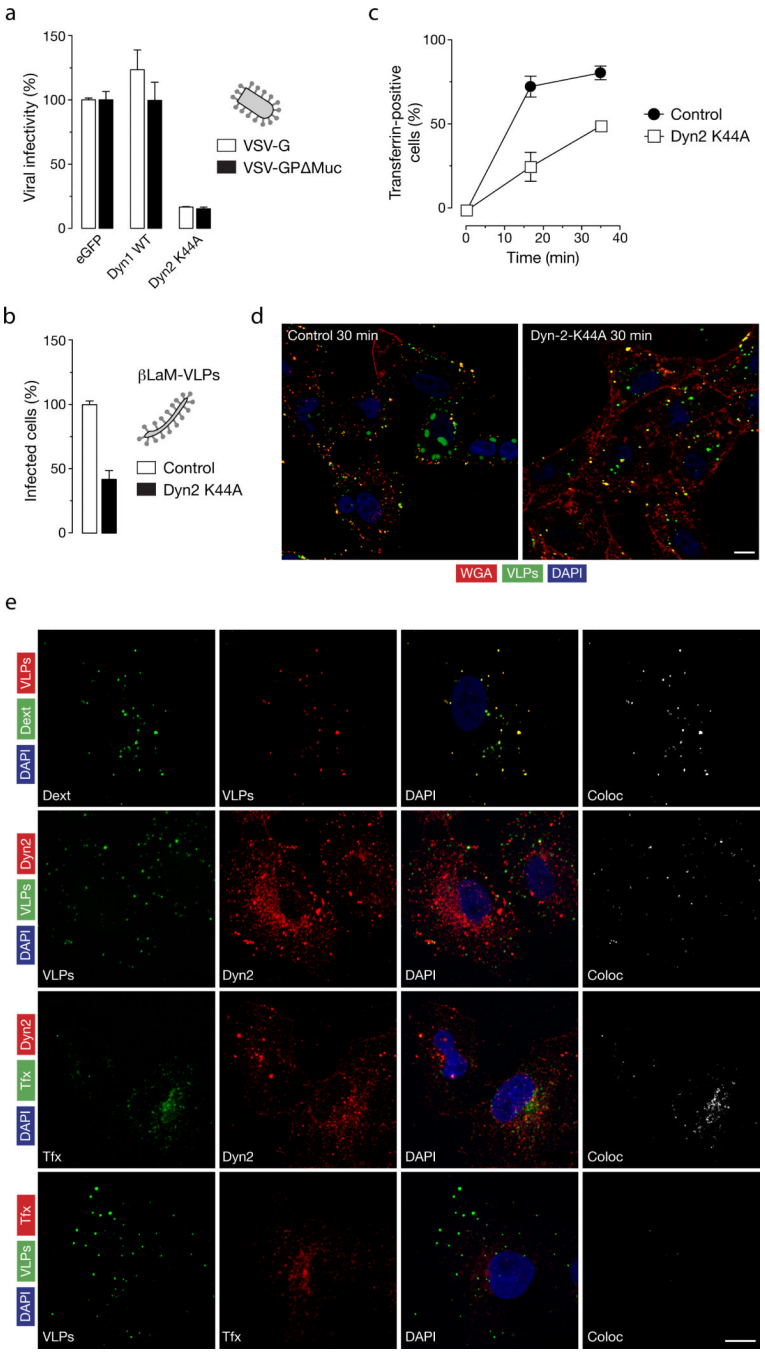

Figure 7. Role of dynamin in EBOV-GPΔMuc-dependent viral uptake and infection

(A) Expression of dominant-negative dynamin-2 inhibits VSV-GPΔMuc infection. Vero cells expressing eGFP or a dominant-negative dynamin-2 protein (Dyn2 K44A) plasmids were exposed to luciferase-expressing VSV-G or VSV-GPΔMuc. FACS-sorted eGFP-positive cells were assayed for luciferase activity to quantitate infection. Infection is normalized to the control vector cotransfected with eGFP for both viruses. (B) Expression of Dyn2 K44A inhibits entry by βLaM-VLPs. Vero cells transfected with either a control vector plasmid or a plasmid expressing Dyn2 K44A were exposed to βLaM-VLPs, and entry was determined by flow cytometry. (C) Dyn2 K44A inhibits transferrin uptake. Vero cells expressing a Dyn2-K44A-eGFP fusion protein were pulsed with 1 μg/mL Alexa-647-labeled

transferrin for the indicated times and VLP uptake was assessed by flow cytometry. (D) Effect of Dyn2 K44A expression on uptake of EBOV VLPs. Representative maximal Z projections of cells transfected with eGFP or Dyn2-K44A-eGFP and exposed to RFP-EBOV VLPs at 37°C for 30 min are shown. Scale bars, 5 μM (E) Endogenous dynamin-2 colocalizes with EBOV VLPs. Vero cells were exposed to the indicated ligands or eGFP/RFP-VLPs for 10 min at 37°C, and then fixed and visualized by confocal fluorescence microscopy. Endogenous dynamin was detected by staining with anti-dynamin primary antibody and an Alexa 594-conjugated secondary antibody. Scale bars, 10 μM. (A-C) Means +/-SD of three replicates are shown.

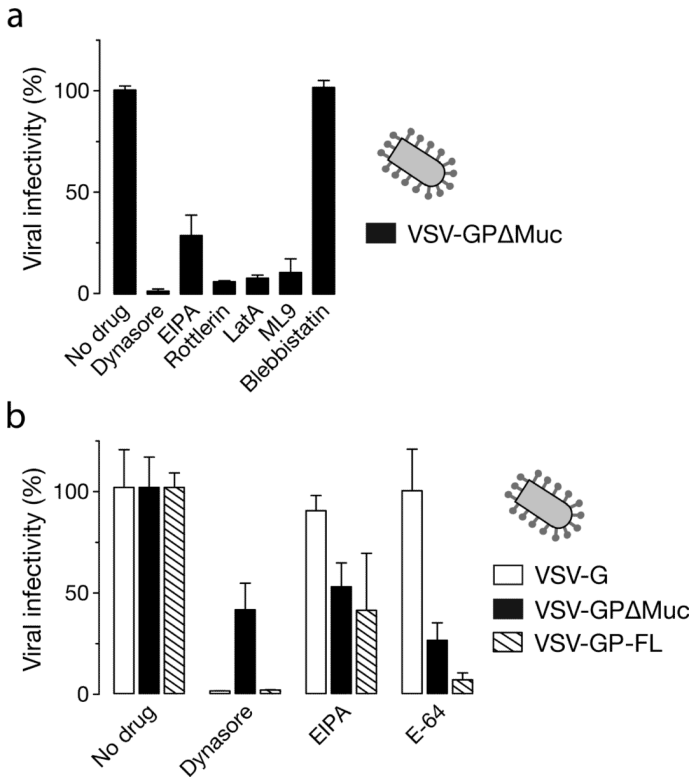

Figure 8. Effects of macropinocytosis and dynamin inhibitors on EBOV GP-dependent infection in monocytes and dendritic cells

(A) Inhibitors of macropinocytosis and dynamin reduce VSV-GPΔMuc infection in the Jaws murine dendritic cell line. Jaws cells were pre-treated with 1% DMSO, 60 μM dynasore, 25 μM EIPA, 2.5 μM rottlerin, 0.01 μM latrunculin A, 5 μM ML9, or 50 μM blebbistatin and then exposed to VSV-GPΔMuc or VSV-G. Infection was scored by counting eGFP-positive cells. (B) Effects of dynasore and EIPA on infection by VSV-GP-FL and VSV-GPΔMuc in adherent PBMCs. CD14-positive PBMCs were pre-treated with 0.5% DMSO, 60 μM Dynasore, 25 μM EIPA, or 300 μM E-64d, and then exposed to virus. Infection was scored by counting eGFP-positive cells. (A-B) Means +/-SD of three replicates are shown.